Available online at www.sciencedirect.com
SCIENCE DIRECT
Biochimica et Biophysica Acta 1753 (2005) 108 – 120
BIOCHIMICA ET BIOPHYSICA ACTA
BBA
http://www.elsevier.com/locate/bba

Structural studies reveal that the diverse morphology of β_2-microglobulin aggregates is a reflection of different molecular architectures

József Kardos [a,b,*], Daichi Okuno [c], Tomoji Kawai [d], Yoshihisa Hagihara [e], Noboru Yumoto [e], Teizo Kitagawa [c], Péter Závodszky [f], Hironobu Naiki [g], Yuji Goto [b]

[a] Department of Biochemistry, Eötvös Loránd University, Pázmány sétány 1/C, Budapest 1117, Hungary
[b] Institute for Protein Research, Osaka University and CREST, Japan Science and Technology Agency, Yamadaoka 3-2, Suita, Osaka 565-0871, Japan
[c] Center for Integrative Bioscience, Okazaki National Research Institutes, Myodaiji, Okazaki 444-8585, Japan
[d] Institute of Scientific and Industrial Research, Osaka University, 8-1 Mihogaoka, Ibaraki, Osaka, Japan
[e] National Institute of Advanced Industrial Science and Technology, 1-8-31 Midorigaoka, Ikeda, Osaka 563-8577, Japan
[f] Institute of Enzymology, Hungarian Academy of Sciences, Karolina ut 29, Budapest, H-1113 Hungary
[g] Faculty of Medical Sciences, University of Fukui and CREST, Japan Science and Technology Agency, Matsuoka, Fukui 910-1193, Japan

Received 15 July 2005; received in revised form 17 August 2005; accepted 19 August 2005
Available online 9 September 2005

Abstract

Amyloid deposition accompanies over 20 degenerative diseases in human, including Alzheimer's, Parkinson's, and prion diseases. Recent studies revealed the importance of other type of protein aggregates, e.g., non-specific aggregates, protofibrils, and small oligomers in the development of such diseases and proved their increased toxicity for living cells in comparison with mature amyloid fibrils. We carried out a comparative structural analysis of different monomeric and aggregated states of β_2-microglobulin, a protein responsible for hemodialysis-related amyloidosis. We investigated the structure of the native and acid-denatured states, as well as that of mature fibrils, immature fibrils, amorphous aggregates, and heat-induced filaments, prepared under various in vitro conditions. Infrared spectroscopy demonstrated that the β-sheet compositions of immature fibrils, heat-induced filaments and amorphous aggregates are characteristic of antiparallel intermolecular β-sheet structure while mature fibrils are different from all others suggesting a unique overall structure and assembly. Filamentous aggregates prepared by heat treatment are of importance in understanding the in vivo disease because of their stability under physiological conditions, where amyloid fibrils and protofibrils formed at acidic pH depolymerize. Atomic force microscopy of heat-induced filaments represented a morphology similar to that of the low pH immature fibrils. At a pH close to the pI of the protein, amorphous aggregates were formed readily with association of the molecules in native-like conformation, followed by formation of intermolecular β-sheet structure in a longer time-scale. Extent of the core buried from the solvent in the various states was investigated by H/D exchange of the amide protons.

Keywords: Amyloid formation; Protein aggregation; β_2-microglobulin; Fourier transform infrared spectroscopy; Secondary structure; Hydrogen-deuterium exchange

1. Introduction

Amyloid fibril deposition of different proteins is associated with nearly two dozen serious diseases, including Alzheimer disease, prion disease, and dialysis-related amyloidosis [1–3]. The increasing wealth of information accumulated in recent years has shown that the ability of amyloid formation is a general property of the polypeptide chains. Numerous proteins and peptides have been shown to be capable of self-assembling into amyloid fibrils in vitro under appropriate conditions, such as low pH, high temperature, or moderate concentrations of salts or co-solvents [1,4,5]. Observation of amyloid fibrils in tissues affected by in vivo diseases suggested that the toxic protein aggregates are mature amyloid fibrils. However, recent experimental data has provided evidence that the pre-fibrillar aggregates, such as protofilaments, or amorphous aggregates

Abbreviations: β2m, β_2-microglobulin; H/D, hydrogen-deuterium; FTIR, Fourier transform infrared; ThT, thioflavin T; AFM, atomic force microscopy; CD, circular dichroism; DSC, differential scanning calorimetry; pD*, pH-meter reading in D_2O solution

* Corresponding author. Department of Biochemistry, Eötvös Loránd University, Pázmány P. sétány 1/C, Budapest H-1117, Hungary. Fax: +36 1 381 2172.
E-mail address: kardos@cerberus.elte.hu (J. Kardos).

1570-9639/$ - see front matter © 2005 Elsevier B.V. All rights reserved.
doi:10.1016/j.bbapap.2005.08.013

might be more toxic to the living cells than long, rigid fibrils [5–9]. These results suggested the importance of the investigation of all different types of aggregates, the mechanism of their formation, and their kinetic and structural relationships on the pathway of amyloid formation.

Hemodialysis-related amyloidosis of β_2-microglobulin (β2m) is a common and serious complication in patients receiving hemodialysis for more than 10 years [3,10]. Carpal tunnel syndrome and destructive arthropathy associated with cystic bone lesions are the major clinical manifestations of β2m amyloidosis [11]. The role of β2m in two diseases unrelated to dialysis: plasma cell-associated systemic amyloidosis and primary localized cutaneous nodular amyloidosis has also been reported recently [12,13]. In the native state, β2m adopts a typical immunoglobulin fold consisting of seven β-strands organized into two β-sheets connected by a disulfide-bridge. The increased concentration of β2m in hemodialysis patients is thought to be responsible for the formation of amyloid fibrils in the musculoskeletal system [10], though the mechanism and nucleation step of this process are not well understood yet. Moreover, β2m forms no fibrils in vitro under physiological conditions even at high protein concentration. However, at low pH, β2m readily forms fibrils in a seed-dependent extension reaction [14–16] or in a self-nucleated manner [17]. Although these fibrils are not stable at physiological pH, and the in vivo relevance of these in vitro produced fibrils are not yet clear, their typical long, straight, amyloid morphology and the fact that fibrils purified from patients can be used as seeds in a fibril extension reaction at low pH [14] indicate a possible relationship.

In addition to the mature fibrils, β2m forms immature fibrils or protofibrils under high salt concentration at pH 2.5 or at moderately low pH values such as pH 3.5 [18,19]. The morphologies of these fibrillar aggregates are known but the organization of the building monomers, the relationship between the morphology and the secondary structure composition and the structural relationship or compatibility between the different types of aggregates are not yet well understood. We found that β2m has a tendency for non-specific aggregation in the pH range of 5–5.5 at 37 °C. Using heat treatment, curvilinear filaments were formed at physiological pH. These filaments are stable under physiological conditions.

Here, we carry out a comparative study of the different aggregated states of β2m as well as the native state and the acid denatured state on the secondary structure composition, morphology, and the extent of the rigid hydrophobic core. We discuss the compatibility of the various structures and the possible in vivo importance of the amorphous aggregates and the novel heat-induced filaments.

2. Materials and methods

2.1. Protein expression and purification

Recombinant β2m was expressed in *E. coli* and purified as described previously [20–22].

2.2. Polymerization reaction and preparation of various types of aggregates

Amyloid fibril formation of β2m at pH 2.5 was carried out by the fibril extension method established by Naiki et al. [23–25], in which seed fibrils at a concentration of 5 μg/ml were extended by 0.3 mg/ml monomer β2m at pH 2.5 and 37 °C. After completion of the reaction (approximately 3 h) fibrils were concentrated by centrifugation (15,000 rpm, 30 min at 4 °C in a Hitachi CF 15R centrifuge).

β2m monomer solutions at a concentration of 5 mg/ml were dialyzed at 4 °C overnight into the following buffers: 50 mM Na-citrate, 100 mM NaCl, at pH 3.5, pH 5.0, and pH 6.0; 50 mM Na-phosphate, 100 mM NaCl, pH 6.0, pH 7.0, and pH 8.0. After dialysis, aliquots of 200 μl of each the samples and buffers were lyophilized. The samples were used for the FTIR spectroscopy studies and H/D exchange measurements at 37 °C. The originally transparent sample at pH 5.0 immediately started to aggregate when it was exposed to 37 °C and within a few minutes, large part of the protein sample was precipitated into white grains.

A β2m sample at pH 7.0 was subjected to a heat treatment for 1 h at 75 °C. After incubation the solution showed opalescent aggregates, which were difficult to spin down completely. A centrifugation at 15,000 rpm for 30 min resulted in only 50% of the protein in the pellet as proved by the concentration of the supernatant. At pH 3.5, the protein solution started to aggregate during the FTIR measurement at 37 °C.

2.3. Thioflavin T fluorescence measurements

Depending on the protein concentration and experiment, an aliquot of 1–5 μl was taken from the sample and mixed with 1.0 ml of 5 μM ThT in 50 mM glycine–NaOH buffer, pH 8.5 [25]. ThT fluorescence was monitored at 485 nm with excitation at 445 nm at 25 °C using an F4500 fluorescence spectrophotometer (Hitachi).

2.4. Atomic force microscopy (AFM)

To image the various aggregates of β2m, the samples were diluted 100-fold with water and, without delay, 10 μl were placed onto freshly cleaved mica and left for 1 min. The samples were then rinsed with deionized water and dried with compressed air. AFM images were obtained using SPI3700-SPA300 dynamic force microscope (Seiko Instruments). The scanning tip used was Si microcantilever (SI-DF20, Seiko Instruments, spring constant = 13 N/m, resonance frequency = 135 kHz). The scan rate was 1 Hz.

2.5. Secondary structure determination by Fourier transform infrared spectroscopy

FTIR measurements were performed on FT-600 (Jasco) and Excalibur 3000 (BioRad) instruments equipped with MCT and DTGS detectors, respectively. To avoid the contribution of water vapor peaks to the spectra, the instruments were purged with N_2 and dry-air, respectively. CaF_2 cells with 50 and 100 μM teflon spacers were used in water-jacketed cell holders at 25 or 37 °C, as measured by a sensor attached to the cell window. The protein concentration of 3–6 mg/ml was relatively low for FTIR, thus the experiments were carried out in D_2O solutions to avoid the high absorbance of H_2O in the amide I range (around 1650 cm^{-1}). Buffers used for the various states of β2m were as follows: 50 mM Na-citrate, 100 mM NaCl, pD 2.5, pD 4.0, pD 5.5, and 50 mM Na-phosphate, 100 mM NaCl, pD 7.5, pD 8.5. pD was defined as pD = pD* + 0.4, where pD*, the pH meter reading in D_2O, is corrected for the isotop effect. Fully deuterated samples of the different aggregates were prepared from fully deuterated native β2m (24 h incubation at 37 °C, in D_2O buffer at pD 8.5).

To estimate the secondary structure, peak fitting of the amide I band (1600–1700 cm^{-1}) by Gaussian-shaped components was performed on the non-deconvoluted spectra. The positions and number of the components were determined from the second derivative analysis of the spectra. To treat the borders of the amide I region appropriately, the fitting was carried out in the

1570–1730 cm^{-1} wave number range. The peak positions were fixed in the fitting. The width of each Gaussian curve was maximized in 20 cm^{-1}. The contribution of each component to the amide I band was evaluated by integrating the area under the curve and then normalizing to the total area of the amide I band. The expectable error of the method is generally around 5%. In some cases, we indicated a possible upper limit for certain components, when the best fitting presented zero contribution of that component.

2.6. Hydrogen–deuterium exchange

H/D exchange kinetics of the amide protons was followed by the change of the amide II infrared absorption band around 1550 cm^{-1}, which corresponds to the bending vibration of the amide proton. The newly formed N–D bond bending vibration appears in the spectrum around 1450 cm^{-1}. Lyophilized samples were dissolved in D_2O within a few seconds and then filled into the CaF_2 cell. The IR spectra (400–4000 cm^{-1} region) were recorded starting 30–50 s after complete dissolution. A background spectrum of the buffer was recorded and subtracted from every sample spectrum. The fraction of the unexchanged amide protons (X) was calculated from the ratio of the amide II/amide I bands considering these values from the spectra of the unexchanged proteins and of the fully deuterated ones as 100% and 0%, respectively. Since we measured different conformational states of β2m having significantly different shapes and maxima of the amide I band, we used the area of this band (1700–1600 cm^{-1} region) instead of the maximum absorption as an inner reference. The amide II band was evaluated from the absorption at the wavenumber of its maximum (1547–1550 cm^{-1}). The peak heights were calculated relative to the baseline absorbances measured at 1789 cm^{-1}. Spectra with amide II absorption of the unexchanged samples were recorded in a mixture of 10% (V/V) H_2O/90% (V/V) DMSO. The low absorption of this solution, compared to pure H_2O, made the background correction easy and accurate even at a protein concentration as low as 5 mg/ml. Note that the secondary structure of β2m and hence the shape of amide I in DMSO is significantly altered. We assumed that the peak area is operationally unchanged and it was in good correlation with the experimental results using the same protein concentration under different conditions. The basics of the H/D exchange experiments and the method of the evaluation were described previously [26–28]. Poly-D,L-alanine was used to follow the H/D exchange of a disordered, exposed structure as a reference [29]. The experiments were carried out at 37 °C, under the buffer conditions described in Section 2.5.

2.7. CD spectroscopy

CD measurements were carried out on a J-720 W spectropolarimeter (Jasco) equipped with a PT-340 temperature control unit. Protein concentrations and buffer solutions were identical to those in the FTIR measurements. A quartz cell of 0.02 cm pathlength was used for recording the spectra in the far UV region. Considering the weakness of the CD spectroscopy in the estimation of β-structure, a specific method was used for the investigation of the heat-treated β2m sample. We used the spectrum of the native, monomeric β2m as a basis spectrum for the native secondary structure of ~47% antiparallel β-sheet, and 40% turn, as obtained from the X-ray structure (PDB entry 1DUZ). The spectra of the mature fibrils at pH 2.5 or immature fibrils at pH 3.5 were used as base spectrum for the intermolecular β-sheet structure of β2m. A third base spectrum of the disordered β2m was measured in the presence of 4 M GdnHCl. β2m is proved to be disordered in 4 M GdnHCl having a far-UV CD spectrum similar to the spectrum in 6 M GdnHCl. Using a 0.02-cm pathlength quartz cell, recording of the CD spectrum was possible down to the wavelength of 202 nm. The linear combination of these spectra was used as a fitting method for the spectrum of the heat-induced filaments.

2.8. Ultracentrifuge analysis

An Optima XL-I analytical ultracentrifuge (Beckman) was used. Sedimentation experiments were carried out in the sedimentation velocity mode at 40,000 and 55,000 rpm. Data obtained were analyzed using Origin 4.0 (MicroCal) and Ultrascan for Linux (SciScan) using the method of Demeler et al. [30]. β2m samples diluted to ~0.5 mg/ml were used. A native, monomer β2m reference was measured in 50 mM Na-phosphate, 100 mM NaCl, at pH 7.0.

2.9. Differential scanning calorimetry

Calorimetric experiments were carried out on a VP-DSC (MicroCal) instrument. Protein concentration was 0.1 mg/ml in 50 mM Na-phosphate, 100 mM NaCl, pH 7.5. Thermal unfolding curves were analyzed by Origin 7.0 for DSC (MicroCal) software.

3. Results

3.1. Various aggregates and soluble forms of β2m

β2m is capable of aggregation and formation of fibrils/protofibrils/amorphous aggregates in a wide range of pH. We carried out comparative work on the various conformational states of β2m to investigate their structural similarities and their possible role in the amyloid formation and its nucleation, exploring the differences between mature fibrils formed at low pH and aggregates that are stable under physiological conditions. Different states of β2m studied in this paper are as follows:

(1) *Mature fibrils* were prepared by seed dependent polymerization at pH 2.5 [23–25] in 50 mM Na-citrate in the presence of 100 mM NaCl.
(2) *Curved, immature fibrils* were formed at pH 3.5–4.0 by slightly modifying the conditions reported by McParland et al. [31] in a buffer of 50 mM Na-citrate, 100 mM NaCl. These two forms of fibrils were quasi soluble and the solutions remained clear and transparent.
(3) It was found that in the pH range of 5.0–5.5 in the presence of 100 mM NaCl at 37 °C, β2m forms *amorphous aggregates* and rapidly precipitates in the test tube at the protein concentration used (3–6 mg/ml).
(4) At physiological pH in a buffer of 50 mM Na-phosphate, 100 mM NaCl, after 1 h incubation at 75 °C, the solution of β2m became opalescent as a sign of intermolecular aggregation. This *heat-induced aggregate* was also subjected to further studies.
(5) At pH 2.5, monomeric β2m is reported to be unfolded in the so called *acid denatured state* [16,32,33].
(6) As a reference we studied the properties of *native* β2m under physiological conditions in the pH range of 7.0–8.0 (see Section 2 for details).

3.2. ThT fluorescence of different aggregated forms of β2m

After 3 days incubation at 37 °C, the samples were subjected to ThT fluorescence assay. The protein concentration used was identical to that of the FTIR, H/D exchange and CD measurements (3–6 mg/ml). Interestingly, all the different aggregates of β2m presented relatively high fluorescence intensity (Fig. 1), with the highest value for mature fibrils. In decreasing order of intensity, the following results were obtained: pH 2.5 mature fibrils > pH 3.5 immature fibrils > heat-treated β2m (pH 7.5) > pH 5.0 aggregates. The samples at pH 2.5 and 3.5 were transparent, while the sample at pH 5.0 and the heat-treated

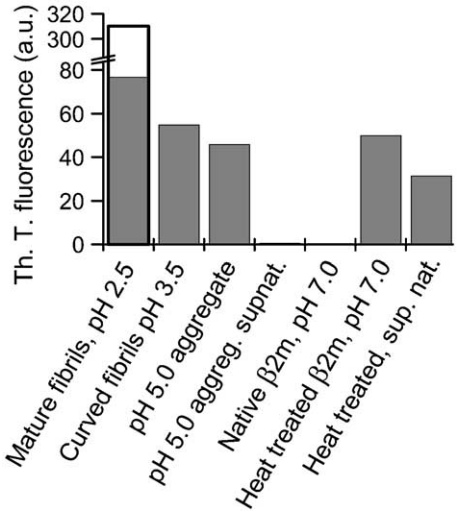

Fig. 1. ThT fluorescence intensity of different types of aggregates of β2m. The highest intensity is exhibited by mature fibrils (pH 2.5), however, all the different aggregates showed significant ThT fluorescence. Supernatants after 10 min centrifugation at 15,000 rpm are also presented in the case of pH 5.0 and pH 7.0 aggregates. The open column shows the normalized intensity of fibrils freshly formed at 0.3 mg/ml concentration.

sample showed precipitation. To separate the contribution of the precipitate and the possible operationally soluble part, we spun down the two opalizing samples at 15,000 rpm for 10 min in a table-top centrifuge. ThT intensities of these supernatants normalized for the remaining protein concentrations were included in Fig. 1. At pH 5.0, 95% of the sample could be spun down with no remaining fluorescence in the supernatant. In contrast to this, only half of the protein content of the pH 7.5 heat treated sample could be spun down and the supernatant showed relatively high ThT fluorescence intensity suggesting the presence of a quasi soluble aggregate with moderate size. As a reference, the native, monomer β2m at pH 7.5 exhibited no fluorescence. It should be noted, that the relative ThT intensity of freshly prepared mature fibrils at 0.3 mg/ml concentration is more than 3 times higher than that of the samples of high protein concentration used in these experiments.

3.3. Atomic force microscopy

Morphologies of the various types of aggregates of β2m were investigated by AFM. The protein concentration and preparation of the samples were identical to those used in other experiments such as FTIR spectroscopy. Images of the different forms of β2m recorded in dry tapping mode are presented in Fig. 2. Morphology and characteristic dimensions are summarized in Table 1. Mature fibrils, formed at pH 2.5, showed typical morphology of long and straight amyloid fibrils. We can distinguish fibrils with different thickness (height) and level of association of protofibrils. 70% of the fibrils exhibited a characteristic height of 10–12 nm, and 30% 7–9 nm. The fibrils showed clear left-handed helical twist. The height was changing within the given range in every single fibril along the axis, depending on the twist. In a few cases, we could observe fibrils with average heights of 15 nm and 5 nm. The 5 nm type ones exhibited no visible twist. The 7–9 nm type and 5 nm type fibrils are similar to those ones observed by Kad et al. [17] in spontaneous fibril formation experiments.

Table 1
Morphology and characteristic parameters of different β2m aggregates investigated by AFM

Condition	pH 2.5, seeded	pH 3.5	pH 5.0	pH 7.5, heat treatment
Morphology	Straight, mature fibrils	Curved, immature fibrils	Amorphous aggregate	Curved filaments
Height (nm)	7–9, 10–12[a]	3–4	No specific size	3–4
Length (nm)	500–2000	50–500	>20	20–100

[a] Because of the twisted helical morphology of mature fibrils we could measure a range of heights periodically changing with the twist along the fibril.

Aggregates at pH 3.5 proved to be curved protofibrils or immature fibrils, with a characteristic height of 3.5 ± 0.5 nm and length of 50–500 nm. These filaments did not show any helical twist. In some images we see a nodular assembly and monomers or dimers of the building "modules" with the same, 3.5 nm height (Fig. 2B). This phenomenon was also reported by Kad et al. [32]. At pH 5.0, we found amorphous aggregates of β2m, with no characteristic size or shape (Fig. 2C).

The heat-treated β2m (pH 7.5) formed short, 20–100 nm long curved filaments with a height of 3.5 ± 0.4 nm, similar to the pH 3.5 aggregates. We could also observe the same morphology concerning the nodular assembly (Fig. 2D).

3.4. Fourier transform infrared spectroscopy

We investigated the secondary structure of the various monomeric and aggregated states of β2m by infrared spectros-

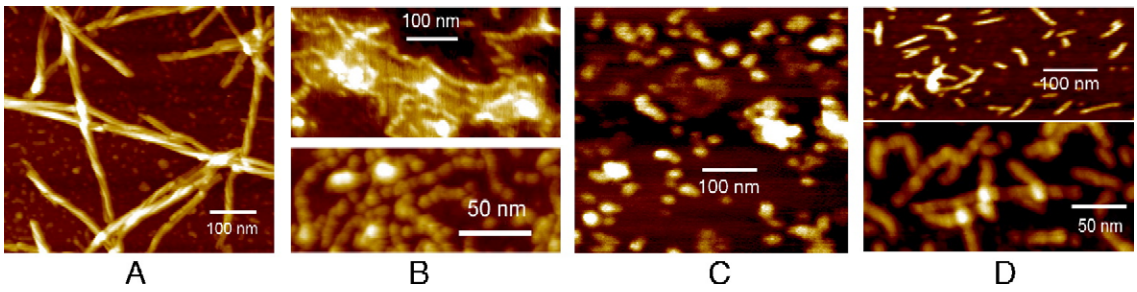

Fig. 2. Morphology of the different aggregates of β2m studied by AFM. (A) Mature fibrils at pH 2.5, (B) Curved filaments (immature fibrils) at pH 3.5, in the lower panel, we can see a nodular organization. (C) Amorphous aggregates, formed at pH 5.0. (D) Heat-induced filaments at pH 7.5.

copy. The amide I band that is mainly due to the C=O stretching vibration of the peptide backbone is sensitive to the secondary structure [34]. The second derivative of the amide I band in the range of 1600–1700 cm^{-1} was used for the determination of the number and the positions of the structural components. In order to get the secondary structure compositions, fittings were performed on the non-deconvoluted amid I spectra keeping the peak positions fixed. We assigned the components in the spectra to the secondary structure as follows: 1635–1640 cm^{-1}, β-sheet; 1690–1695 cm^{-1} with no H/D exchange and 1682–1685 cm^{-1} in deuterated form, high frequency contribution of antiparallel β-sheet; 1617–1626 cm^{-1} intermolecular β-sheet; 1642–1646 cm^{-1} disordered structure; 1650–1660 cm^{-1}, α-helix; 1660–1675 cm^{-1} β-turn [34–38]. The range of 1600–1613 cm^{-1} was assigned to side chain contributions [39]. Because the 3–6 mg/ml protein concentration we used is relatively low for FTIR experiments, the measurements were carried out in D_2O solutions. After dissolution in D_2O buffer, the labile protons of the protein molecule start to exchange with deuterons upon exposure to heavy water. This results in a slight shift in the position of the components of the amide I band as a consequence of the isotopic effect through the hydrogen/deuterium bonding alterations, without any conformational change [40]. This shift was carefully examined, repeating the experiments with fully deuterated samples helping to identify and distinguish the secondary structure elements. Fig. 3 presents the amide I bands and their second derivatives of the various forms of β2m. The secondary structure estimates of the different forms of β2m are shown in Table 2.

Native β2m presented a sharp β-sheet component around 1638 cm^{-1} at the beginning of the H/D exchange (not shown), which is shifted to 1635 cm^{-1} in the fully deuterated sample (Fig. 3A). Analysis of the spectrum showed approximately 50% β-sheet similarly to the X-ray structure (47% antiparallel β-sheet, 40% turn, 1duz.pdb). The high frequency β-sheet component that distinguishes the antiparallel β-sheet from the parallel one [41] is well expressed at 1682 cm^{-1} in the deuterated amide I′. Two components represent β-turn content at 1662 cm^{-1} and 1669 cm^{-1}.

After heat treatment (75 °C, 1 h) at pD 7.5, the β2m solution became slightly opalized. The infrared spectrum showed appearance of a peak at 1617 cm^{-1} together with the high frequency antiparallel β-sheet component at 1685 cm^{-1}, suggesting the formation of antiparallel intermolecular β-sheet structure [42,43] in the aggregate. The intramolecular β-sheet component of the native protein at 1635 cm^{-1} was still present with a lower contribution (Fig. 3A). This suggested either the possible presence of native molecules in the solution or the presence of a native-like β-sheet structural component in the curved filaments. The secondary structure fitting proved that the heat-induced aggregate sample has no or small (<5%) random content (Table 2).

At a protein concentration as high as 5 mg/ml, β2m readily forms large precipitates at pD 5.5 in the presence of 100 mM NaCl at 37 °C (see Section 2 about the preparation of the sample). The remaining soluble protein concentration after 3 days incubation at 37 °C was approximately 0.3 mg/ml as

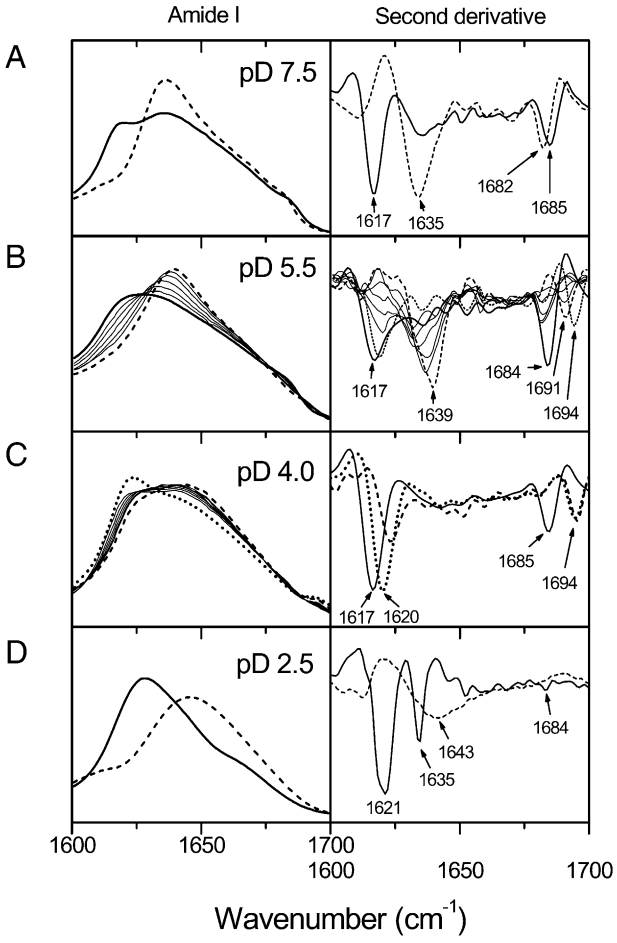

Fig. 3. Infrared spectra of the different forms of β2m. Left: amide I bands, right: second derivatives of the amide I. (A) Heat treated sample (solid line), and native β2m (dashed) at pD 7.5 in the fully deuterated form. (B) Amorphous aggregates at pD 5.5. After dialysis at 4 °C the sample was heated up to 37 °C for 5 min and then spun down for 2 min at 14,000 rpm. The pellet was dissolved in the same buffer and filled into the CaF_2 cell with no delay. Dashed line shows the first, native like spectrum, thin lines present the further conformational change in 10 h time, and the solid thick line shows the spectrum of a sample measured after 3 days incubation at 37 °C. Dotted line in the second derivatives shows a sample incubated in H_2O buffer at 37 °C for 3 days and exposed to H/D exchange for 10 h in D_2O buffer. (C) Formation of curved filaments at pD 4.0: (dashed) amide I and its second derivative of the sample after 10 min incubation at 37 °C, (thin solid lines) spectral changes in the amide I in 10 h course of aggregation, (dotted line) 3 days preincubation at 37 °C in H_2O buffer followed by 10 h of H/D exchange in D_2O buffer, (thick solid line) second derivative of a sample prepared from fully deuterated β2m. (D) Acid denatured state at pH 2.5 (dashed) and fully deuterated mature fibrils (solid).

confirmed by centrifugation at 15,000 rpm for 30 min in a tabletop centrifuge. The FTIR analysis suggests that the precipitation precedes the large changes in the structure. Immediately after precipitation at 37 °C, the IR spectrum shows native-like shape with a slightly shifted main component in the second derivative at 1639 cm^{-1} (Fig. 3B) or at 1636 cm^{-1} in a fully deuterated protein sample (not shown). This component could not arise from the contribution of native soluble β2m molecules coexisting with the precipitates because after 5 min aggregation at 37 °C the sample was spun down and the pellet was used for the FTIR measurements. The spectral analysis showed increased turn and disordered

Table 2
Secondary structure estimation of various conformations of β2m as obtained from the FTIR spectral analysis[a]

	β-sheet		Random/ Others (%)	Turns (%)
	Inter-	Intra-		
	Molecular (%)			
Native, pD 7.5	0	51	8	40
Heat-induced aggregate, pD 7.5	9	50	<5[b]	39
pD 5.5 aggregate 10 min	3	30	21[c]	47
pD 5.5 aggregate 3 days	32	25	<5[b]	37
Immature fibrils, pD 4.0	36	8–18	5–15	40
Acid denatured state, pD 2.5	0	<5[b]	50–60[d]	25–35
Mature fibrils at pD 2.5	53	15	4	27
X-ray structure (1DUZ)	0	47	13	40

[a] For assignment of the spectral components to the secondary structure, please, refer to Section 3.4.
[b] A possible upper limit.
[c] Random and α-helix cannot be separated.
[d] Mainly random, some helix cannot be excluded, the spectral fitting has some uncertainty because of the broad components.

structure and decreased β-structure content (Table 2). During further incubation at 37 °C an intermolecular β-sheet component appeared around 1620 cm^{-1} (1617 cm^{-1} in the fully deuterated sample) while the random and turn content were decreasing. The presence of the high frequency β-component indicates the antiparallel nature of the intermolecular β-structure (see Table 2 and Fig. 3B). The increased local protein concentration in the interior of the large aggregates might promote the conformational change and the formation of the intermolecular β-sheet structure. Table 2 presents the secondary structure elements after 3 days incubation. Intriguingly, the β-sheet content is higher than in the native molecule, similar to that of the mature fibrils, though it is contributed by two markedly different components, an intermolecular and a native-like intramolecular antiparallel β-sheet.

Curved protofibrils at pD 4.0 exhibit an intermolecular β-sheet component at 1617 cm^{-1} in the deuterated form similarly to the heat-induced filaments and the amorphous aggregates (Fig. 3C). The high frequency antiparallel β-component is also well expressed. The random content of this form is higher than that of the mature fibrils. (Fig. 3, Table 2).

Monomer β2m is essentially disordered at pD 2.5. Characteristic component in the spectra is the random structure with a contribution of 50–60%, showing no or extremely low β-sheet content (Fig. 3D, Table 2). The components of the spectrum are broad and not well separated, also suggesting a flexible, fluctuating, disordered structure. It was difficult to separate a possible α-helical contribution from the random component.

At pD 2.5 mature fibrils presented 68% β-sheet content. It's major feature is the approximately 53% low frequency β-component, which corresponds to the intermolecular β-structure, appearing at an evidently higher wavenumber of 1621 cm^{-1} (deuterated form), compared to the 1617 cm^{-1} in the other aggregates (Fig. 3A–C). The shape of the peak suggests that it is not a clear single component, rather a sum of close components. In the undeuterated form of mature fibrils a similar double or composite peak can be observed around 1624 cm^{-1} (data not shown). The high frequency β-sheet component (Fig. 3A–C) is mainly missing, suggesting that the intermolecular β-structure of the mature fibrils is significantly different from that of the other aggregates (Fig. 3D). This property supports the idea of the parallel organization of the strands in the intermolecular β-sheet of the mature fibrils because a high frequency β-component may arise only from antiparallel β-structure [37]. The small, hardly observable component at 1684 cm^{-1} may rather be coupled to another, smaller but sharp component in the β-structure region at 1635 cm^{-1} with 15% contribution suggesting antiparallel β-sheet structure. However, it is questionable whether it represents a native-like intramolecular β-sheet (compare Fig. 3A–D) or some extended structure.

3.5. Hydrogen–deuterium exchange

The extent of the rigid hydrophobic core in different states of β2m was investigated by H/D exchange kinetics of amide protons. The amide II infrared band of proteins is mainly contributed by the N–H bending vibration of amide groups located around 1550 cm^{-1}. Depending on the H-bond structure and dynamic properties of a polypeptide chain the amide protons become exposed to the D_2O solution resulting in H/D exchange and decrease of the amide II. Although FTIR spectroscopy used in this work is not able to distinguish individual amide protons, large molecules and aggregates can be directly investigated. β2m has 110 amide protons including protons of five Asn and three Gln side-chains. Fig. 4A presents changes in the amide II band corresponding to H/D exchange. The undeuterated β2m reference was measured in 90% (V/V) DMSO/10% (V/V) H_2O mixture to avoid the strong absorption of H_2O that makes baseline subtractions difficult (Fig. 4B, see Section 2.6 for further details). The exchange kinetics of the native β2m at pD 8.5 and 7.5 was rapid and at least 95% complete within 3 and 10 h, respectively (Fig. 5A). This alteration in the exchange rate of the native β2m arises from the pH dependence of the intrinsic chemical exchange rate: The intrinsic exchange rate reflects the exchange of an amide proton fully exposed to the solvent [29]. Note that McParland et al. [31] reported a slower exchange rate of the native β2m from one dimensional NMR, which could arise from the more than one order of magnitude lower chemical exchange rate in their experiment at 15 °C. In our previous works, the H/D exchange of individual amide protons of native β2m were followed by the intensity changes in the HSQC NMR spectra [20,22,33]. Rapid exchange was observed with two third of the residues disappearing during the dead time of the measurement at 5 °C at pD* 6.5 [20,33]. After 24 h incubation, approximately 30 amide protons of decreased intensity were still visible. Taking into account the approximately 150 fold higher chemical (intrinsic) exchange rate at 37 °C and pD 7.5, the equivalent exchange time is 10 min in our present work. The unexchanged 23% of the amide protons of native β2m after 10 min is in good agreement with the NMR results.

Heat-induced filaments showed increased amide proton protection against H/D exchange indicating the presence of a rigid, probably H-bonded core (Fig. 5A). After 4 h, the

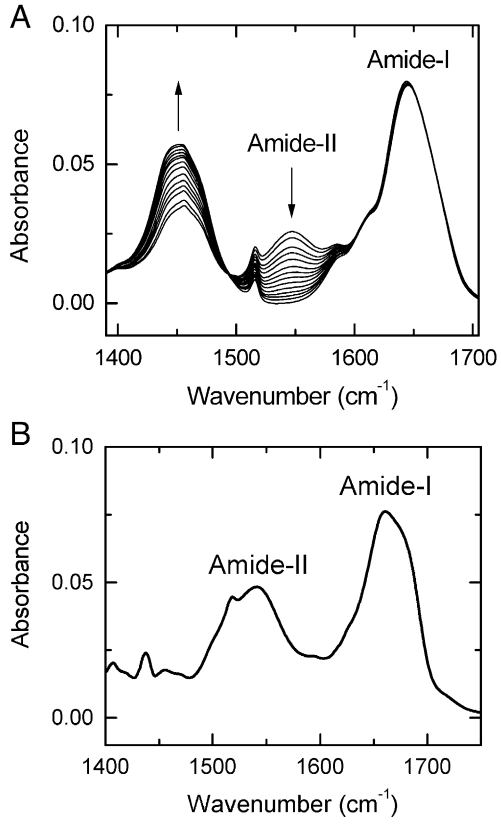

Fig. 4. (A) H/D exchange measurement of acid denatured monomeric β2m in 50 mM Na-citrate, 100 mM NaCl, at pD 2.5. Arrows show the direction of changes in the infrared spectra. With exchanging the amide protons to deuterons the amide II band around 1550 cm^{-1} is disappearing. For further details, see Section 2.6. (B) Infrared spectrum of unexchanged β2m in 90%(V/V) DMSO/10%(V/V) H_2O buffer mixture was used as 100% reference in the calculation of the fraction of unexchanged amide protons.

exchange reaction virtually stopped with 17% of remaining unexchanged amid protons.

Amorphous aggregate samples prepared by 3 days incubation at pH 5.0 at 37 °C exhibited high protection for H/D exchange compared to the non-incubated sample (Fig. 5B). This protection, extended to approximately 60% of the amide protons may be caused by the slow penetration of D_2O into the interior of the large precipitates and/or the protection of amide protons through H-bonding. The position of the antiparallel β-sheet component at 1693 cm^{-1} was constant during the 10 h of H/D exchange experiment suggesting that the amide protons in this structural element are protected from H/D exchange. This component appeared at 1682 cm^{-1} in a sample prepared from fully deuterated β2m (Fig. 3B). There was also some protection visible in the non-incubated samples that could have arisen from the co-occurrence of the formation of intermolecular β-sheet with the H/D exchange at 37 °C. The transfer of the high frequency β-component from 1691 cm^{-1} to 1682 cm^{-1} in the non-incubated sample during the course of the measurement suggests that the intramolecular β-sheet of the native-like conformation in the aggregates was not protected completely from H/D exchange (Fig. 3B) or the amide protons become transiently exposed to the solvent upon the transformation into intermolecular β-sheet.

Immature fibrils prepared by 3 days incubation at 37 °C at pH 3.5 subjected to H/D exchange in D_2O (pD 4.0) showed a rigid core extended to approximately 20% of the amide protons while the sample without preincubation exhibited no significant protection (Fig. 5C). Yamaguchi et al. [44] investigated the H/D exchange kinetics of salt induced immature fibrils having similar morphology to the immature fibrils formed at pH 3.5. Taking into account the different pD values, the 20% unexchanged amide protons after 10 h exchange in the present work is equivalent of the approximately 21% remaining sum of the intensities in the HSQC NMR spectra after 200 h reaction in Yamaguchi's work [44]. The two consistent results suggest that the structure of the β2m aggregates formed at pH 3.5 might be similar to that of the salt induced immature fibrils formed at pD* 2.5.

The second derivative of the amide I of the pH 3.5 immature fibrils (Fig. 3C) shows the presence of an H/D exchange resistant high frequency antiparallel β-sheet component at 1694 cm^{-1} that appears at 1685 cm^{-1} in a sample prepared from fully deuterated protein. Moreover, the low frequency intermolecular β-sheet component is detected around 1620 cm^{-1} during the course of the H/D exchange experiment, while it appears at 1617 cm^{-1} in a fully deuterated sample. This indicates that the amide protons protected from exchange are the ones taking part in the H-bond frame of the intermolecular β-sheet structure of the immature fibrils.

At pD 2.5 monomeric, acid denatured β2m showed no protection against H/D exchange. Despite the low chemical exchange rate at pD 2.5 the reaction was completed in 90 min (Fig. 5D). Poly-D,L-alanine was measured as a disordered reference and showed slightly faster exchange kinetics than that of β2m, possibly arising from the lack of any shielding effect of larger side-chains. Mature fibrils showed high protection that may extend to 50% of the exchangeable N–H protons (Fig. 5D). Analysis of the amide I showed that the intermolecular β-sheet component appeared around 1624 cm^{-1} upon H/D exchange and was protected from that. This component appears at 1621 cm^{-1} in the fully deuterated form of β2m fibrils (Fig. 3D). Previously we reported the H/D exchange of β2m amyloid fibrils followed by two-dimensional NMR spectroscopy collecting sequence specific information by quenching the exchange process and depolymerizing fibrils through dissolution in DMSO [20]. Our present results are consistent with the H/D exchange of acid denatured β2m and mature fibrils at pD 2.5 presented in that work [20]. The same NMR techniques was used in a recent work [44] for the study of the H/D exchange of mature fibrils under experimental conditions similar to our present work (pD* 2.5, 37 °C). Summing up the remaining relative peak intensities in the HSQC spectrum after 10 h exchange resulted in approximately 49% unexchanged amide protons in good agreement with the result of 50% in the present work.

3.6. CD spectroscopy

Fig. 6 presents the CD spectra of various conformations of β2m. Since CD spectroscopy is not able to examine large,

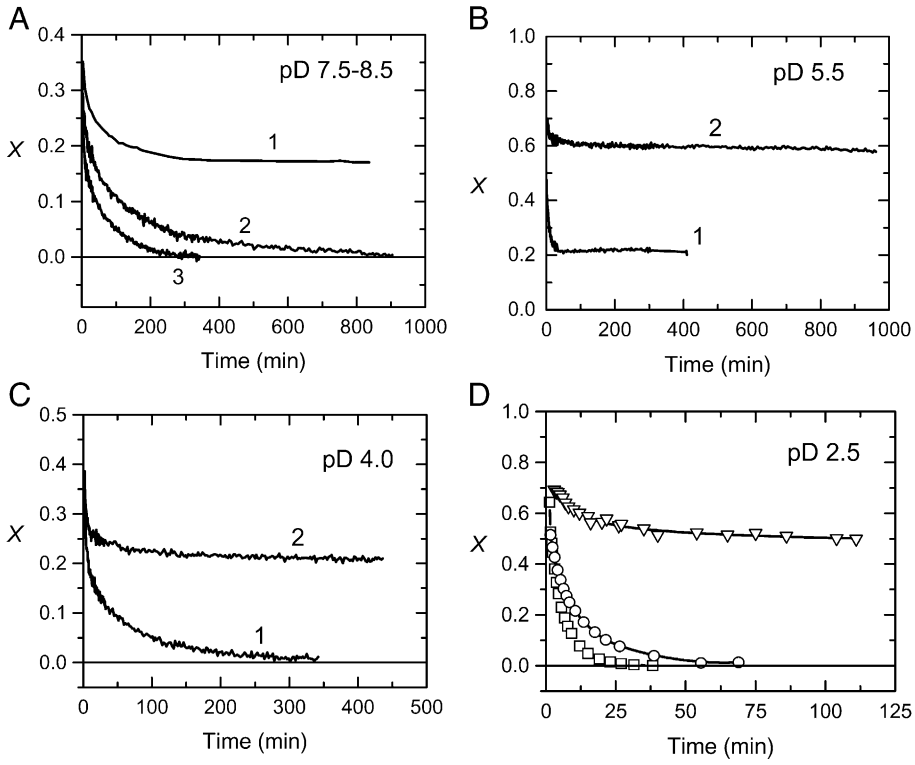

Fig. 5. H/D exchange kinetics of different forms of β2m. *X* is the fraction of the unexchanged amide protons. (A) H/D exchange of heat-induced filaments at pD 7.5 (1), native β2m at pD 7.5 (2) and at pD 8.5 (3). (B) Amide proton exchange at pD 5.5 with no preincubation (1), and with 3 days incubation at 37 °C prior to the measurement (2). (C) Exchange at pD 4.0 without (1), and with 3 days preincubation resulting in immature fibrils at 37 °C (2). (D) Mature amyloid fibrils (triangle), monomeric acid-denatured state of β2m (circle), and poly-D,L-alanine reference (square).

insoluble aggregated particles, aggregates at pH 5.0 were excluded from the experiments. We compared the CD spectra of the heat-treated sample and its supernatant after 10 min centrifugation at 15,000 rpm. Despite the fact that the protein concentration decreased approximately by one half in the supernatant, we found the two spectra virtually identical (not shown). This observation can be explained by the non-transparent nature of larger aggregates for the UV light.

Intriguingly, CD spectrum of the heat treated sample showed ordered structure with no significant disordered component and its shape was somewhat similar to the spectrum of the native protein (Fig. 6A). Our hypothesis was that the solution might be a mixture of native monomers and aggregated protein. To check this idea, we fit the spectrum of the heat treated sample with the linear combination of the spectra of the native monomer β2m, disordered β2m in 4 M GdnHCl, and immature fibrils (pH 3.5), as base spectra. We chose the spectrum of the immature fibrils because of their similar morphology proven by AFM. The best fitting resulted in the combination of 73% native, and 27% immature fibrils with no contribution of the disordered basis spectrum (Fig. 6B). These results suggested that the protein solution is a mixture of native monomers and fibril-like aggregates with low random-coil content. The monomer/fibril composition of this sample was investigated further by analytical ultracentrifuge and differential scanning calorimetry.

We tried to estimate the secondary structure of the various aggregated states and the native β2m as well, using well-known fitting methods for the far-UV CD spectra provided by the Dicroprot package [45]. A good fitting was achieved by the self-consistent method [46] for the native β2m, however, none of the different methods was capable of estimation of the secondary structure of β2m fibrils, immature fibrils, or filaments. Generally, fibrils exhibit a high negative maximum in the spectra at 217 nm, that is higher than that of usual globular proteins with high β-structure content. This leads to the mistaken estimation of significant α-helical content (20–40%), since α-helix has higher CD signal than β-sheet. We can exclude the existence of this structure in this quantity on the basis of the FTIR measurements.

3.7. Ultrancentrifuge analysis

The molecular size distribution and homogeneity of the immature fibrils and the heat treated β2m solution were investigated by analytical ultracentrifuge. Immature fibrils prepared at pH 3.5 were completely spun down at 40,000 or 55,000 rpm with no sign of remaining fraction of monomeric β2m or small oligomers. In contrast, they proved to be operationally soluble using a tabletop centrifuge at 10,000 rpm, suggesting the absence of significant amount of precipitated amorphous aggregates.

We investigated the size distribution of the heat treated β2m sample. First, the sample was spun down for 20 min at 15,000 rpm in a tabletop centrifuge to get rid of the larger size

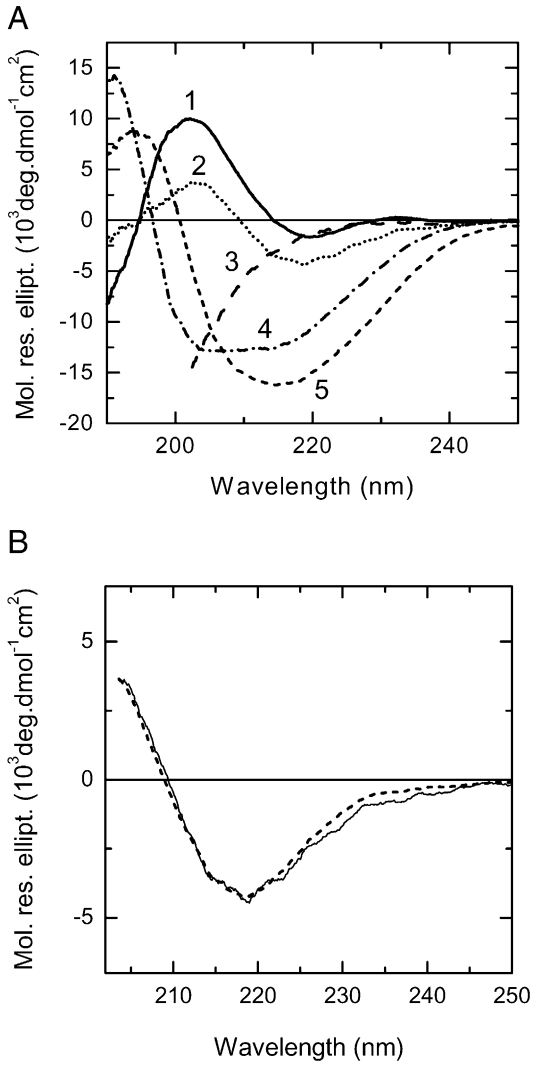

Fig. 6. CD spectra of various forms of β2m. (A) Native state (1); pH 7.0, heat-induced filaments (2); β2m in 4M GdnHCl pH 7.0 (3); immature fibrils at pH 3.5 (4); and mature fibrils at pH 2.5 (5). (B) Structure estimation for the spectrum of the heat-induced filaments (—). Best fitting with the linear combination of 73% native and 27% immature fibril content (- - -).

aggregates that made up half of the protein sample. The supernatant was used for sedimentation velocity analysis at 55,000 rpm. The native, monomer β2m reference sample showed a sedimentation coefficient of 1.6 S. The heat-treated β2m sample presented two sharply separated components, one is similar to the native protein (1.6 S), while the other component exhibited a sedimentation coefficient of approximately 10 S. There was no sign of dimers or smaller oligomers in the sample. The contribution of the two components to the absorbance of the sample suggests that 70% of the sample was native β2m and 30% consisted of the heat-induced short filaments. We tried to estimate the average molecular mass of the filaments, performing simulations in the Ultrascan software, using the data for the average size and width obtained from the AFM experiments. Assuming an axial ratio of 10 for the shape (3.5 nm width, 35 nm length), and a sedimentation coefficient of 10 S, we obtained the average mass of ~300 kDa which is approximately a 30-mer polymer of β2m.

3.8. Differential scanning calorimetry

Thermal denaturation of native β2m at neutral pH at a concentration of 0.1–0.2 mg/ml proved to be 85% reversible as checked by the decrease of the unfolding enthalpy of the transition in the second scan (Fig. 8). The heat-treated sample at pH 7.5 showed a native-like peak with lower size. The peak size showed a good correlation with the monomer content, as estimated from the sedimentation analysis and from the CD measurements.

4. Discussion

In vivo, β2m amyloidosis is developed under physiological conditions. Although β2m is capable of aggregation and formation of fibrils/protofibrils in vitro in a wide range of conditions [14–19,31,32], these conditions are acidic and far from the physiological environment of the human body. While β2m amyloidosis in the patients is an obvious consequence of the increased concentration of β2m upon kidney dialysis, several known and unknown factors co-exist in the development of the disease, such as the length of dialysis, the age of the patient, the type of dialysis membrane used, and there are some experimental evidences on the possible effect of posttranslational modifications and auxiliary proteins [10,43,47–52].

4.1. Variety of morphologies of β2m aggregates

We carried out a comparative work on the different conformational states of β2m, such as the native, monomer form at physiological pH, the acid-denatured monomer state at pH 2.5, the mature fibrils at pH 2.5, immature fibrils at pH 3.5–4.0, amorphous aggregates at pH 5.0–5.5 and heat-induced aggregates at pH 7.0–8.0. The aim of this paper was to explore the structural background of the diverse morphology of β2m aggregates prepared under various conditions and study their role in the amyloid formation of β2m.

All the different type of aggregates exhibited significant ThT fluorescence intensity suggesting the presence of intermolecular β-sheet structure (Fig. 1). Though mature fibrils presented the highest fluorescence intensity, this intensity is only one third of that of freshly prepared fibrils according to the procedure of Naiki and Gejyo [25]. ThT fluorescence intensity of β2m upon spontaneous fibril formation reported by McParland et al. [31] did not change significantly in the pH range of 1.5–4.5. Others reported sharp selectivity of ThT for mature fibrils vs. other aggregates [15,16,32]. The possible explanation of our result is the high protein concentration used in the experiments of the present work.

The characteristic morphologies of the different aggregates were explored by AFM imaging (Fig. 2, Table 1). At pH 2.5, β2m formed long, straight fibrils with left handed twist. We may observe some subclasses of the fibrils with different numbers of protofibrils associated (Table 1). A discussion of the various subclasses of the mature fibrils is beyond the scope of the present work, and is given elsewhere [53]. Immature

fibrils at pH 3.5 and the heat-treated sample at pH 7.0 exhibited similar, curvilinear morphology (Fig. 2B and D). At pH 5.0, β2m formed amorphous aggregates with no characteristic size and shape.

4.2. Structural background of the diverse morphology of β2m aggregates

We investigated the structure of the different forms of β2m by FTIR spectroscopy. The advantages of this technique for the investigation of the secondary structure of proteins are the sensitivity for the detection of β-sheet structure and the possibility of the direct study of protein aggregates. The amide I band is mainly contributed by the C═O stretching vibration of the amide group and is sensitive to the secondary structure and H-bond network of the proteins. We estimated the secondary structure compositions of the various conformational states of β2m determining the components by second derivative analysis and fitting Gaussian curves to the amide I′ bands (Table 2). Native β2m presented antiparallel β-sheet structure with well-expressed high frequency β-component (Fig. 3A). All the aggregates presented ordered secondary structure with low random content. Curved fibrillous aggregates of β2m at pH 3.5 and pH 7.0 exhibited a similar intermolecular β-sheet structure characteristic to antiparallel β-sheet with the same low frequency component at 1617 cm^{-1} and a high frequency component at 1685 cm^{-1} in the deuterated forms (Fig. 3A, C).

Close to its isoelectric point at pH 5.0–5.5, β2m precipitates rapidly at 37 °C retaining a native-like, partially unfolded conformation (Fig. 3B). This "sticky" intermediate might be an amyloid precursor state of β2m and play a role in the nucleation of the aggregation/fibril formation process near to or at neutral pH. The existence of such partially unfolded conformation of β2m under physiological conditions was reported by Chiti et al. [54] and De Lorenzi et al. [55]. After the precipitation of β2m at pH 5.0, an intermolecular β-sheet structure similar to that of the curved, filamentous aggregates (pH 3.5, immature fibrils and pH 7.0, heat-treated sample) is formed in a longer time-scale (Fig. 3B).

4.3. Mature fibrils exhibit a unique β-sheet composition

Mature fibrils presented a characteristic spectrum different from all the other aggregates with a low frequency β-sheet component around 1621 cm^{-1} in the deuterated form suggesting a different hydrogen-bonding pattern. No high frequency component was coupled to this intermolecular β-sheet, raising the possibility of the parallel organization of the β-sheet structure. A second, smaller but sharp component at 1635 cm^{-1} wavenumber suggests the presence of another, likely intramolecular β-sheet component. The small peak at 1684 cm^{-1} in the second derivative spectrum might be its high frequency pair suggesting the antiparallel nature of this β-sheet or might be the contribution of some contamination of other type of aggregates in the sample. Another possible structural assignment of the 1635 cm^{-1} component is an extended chain structure but it is unlikely that the polypeptide chain takes up an extended conformation without β-sheet formation in the fibrils. The significantly altered β-sheet composition of the mature fibrils compared to the other forms of β2m may explain the inefficient seeding function of the curved, immature fibrils, or other aggregates at pH 2.5 as reported previously [32,33]. Instead of the curved immature fibrils, the protofibrils of mature fibrils might be the 5-nm thick fibrils which we could observe rarely in the AFM study of the mature fibril sample. Kad et al. observed this 5 nm thick type of fibril as the first fibrous form in a spontaneous fibril formation experiment [17]. The acid-denatured monomer state of β2m presented a mainly disordered structure with a broad IR band around 1643 cm^{-1} (Fig. 3D, Table 2). The fast H/D exchange rate of the acid denatured β2m also verifies this conclusion. The fact that the extension reaction in the presence of seeds of previously formed fibrils is optimal at pH 2.5, where the monomer state is mainly disordered, suggests that the complete rearrangement of the native structure is necessary for the formation of mature fibrils. Indeed, the β-sheet composition of the mature fibrils is significantly different from that of the native state of β2m, see above (Table 2).

Whether these observations on the relationship between structure and morphology of different β2m aggregates are general for the aggregation and fibril formation of different peptides and proteins remains a question. It is supported by experimental evidences on the parallel β-sheet organization of straight rigid fibrils of Alzheimer's amyloid peptides (1–40) and (10–35), and a peptide from the yeast prion Sup-35 [56–58]. Zurdo et al. [59] reported that the antiparallel high frequency β-sheet component was decreasing upon the formation of straight, twisted mature fibrils of an SH3 domain and suggested that a conversion from antiparallel to parallel organized β-strands could be involved in the substantial structural rearrangement of the polypeptide chain upon amyloid fibril formation. Gordon et al. showed that depending on the amphiphilicity, similar amyloidogenic peptides may take up either antiparallel or parallel β-sheet structure [60].

4.4. The extent of the rigid core in the different forms of β2m

The extent of the rigid, hydrophobic core of the different aggregates was studied by H/D exchange of the amide protons. All the aggregates, even the short curved filaments exhibited significant protection against H/D exchange (Fig. 5). Approximately 50% of the amide protons were protected in the mature fibrils, compared to 20% in the more flexible curved immature fibrils (Fig. 5D, C). The spectral changes in the amide I bands upon the H/D exchange evidenced that protected amide protons are the ones participating in the intermolecular β-sheet structures of the different aggregates. The extent of protection correlates with estimated values of the intermolecular β-sheet content of the mature and immature fibrils (Table 2). These results indicate that in mature fibrils the intermolecular interactions are extended over the larger part of the 100 residues β2m molecule, as it was suggested previously [20], involving the 25–80 middle region which is closed into a ring

by the 25–80 disulfide bridge. This disulfide is essential for the amyloid formation of β2m as we reported in earlier works [16,18,33]. In the case of immature fibrils at pH 3.5, besides the different β-sheet architecture, the lower extent of the rigid, protected core may also explain the more flexible and curved morphology. The protection for H/D exchange in the pH 5.0 amorphous aggregate may be complicated by the difficulty of D_2O penetration into the interior of the large precipitates, therefore may not be appropriate. The solution of the heat-treated sample proved to be a mixture of native molecules, curved filaments and precipitates, as we discuss below, that made the separation of the different contributions difficult.

4.5. Aggregates under physiological conditions

Far-UV CD spectra of the aggregates supported the results of the FTIR studies that the aggregates take up different ordered structures with low random-coil content (Fig. 6). After removing the precipitates, CD spectra of the heat treated sample suggested that it is a mixture of native β2m and heat-induced filaments observed by AFM, and could be successfully fit by a linear combination of the spectra of the native β2m (73%), and immature fibrils (27%). Further studies of the heat-treated sample by analytical ultracentrifuge (Fig. 7) and DSC (Fig. 8) proved that indeed the sample is a mixture of native monomer molecules and filaments. Presence of small oligomers were not detectable, i.e., those were not stable at room temperature or at 37 °C. This shows the importance of the nucleation step in the aggregation process under physiological conditions, where the native monomer β2m cannot form such aggregates spontaneously, even at high protein concentrations. In other words, the partial unfolding of β2m into an "amyloidogenic" conformation is required but not sufficient for the formation of the amyloid fibrils under physiological conditions, where the native state of the protein has significant thermodynamic stability. In consonance with this, immature fibrils that exhibit similar morphology and secondary structure to the heat-induced filaments were spontaneously formed at pH 3.5, where the native state is unstable. Recently it was reported that β2m forms fibrils in the presence of sodium dodecyl sulfate, which may destabilize the structure of the native state [61,62]. Kihara et al. emphasized the importance of the nucleation step in the fibril formation under physiological conditions [62].

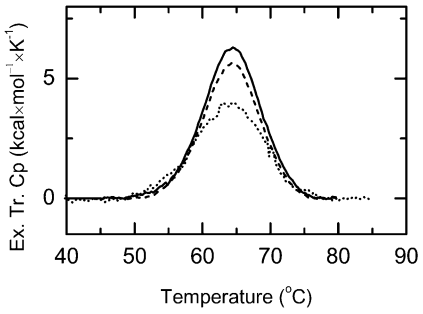

Fig. 8. Differential scanning calorimetry of 0.1 mg/ml native β2m (—) at pH 7.5 and the supernatant (10 min centrifugation at 15,000 rpm) of the heat treated β2m sample diluted to 0.1 mg/ml (•••••). To check the reversibility, native β2m sample was cooled down after the unfolding transition with no delay and a second scan was recorded (- - -).

4.6. Non-interconvertible structures indicate distinct pathways

In conclusion, we showed evidence that the morphology of the various aggregates of β2m is a consequence of the different organization at the molecular, atomic level. Our findings are not consistent with a model where the difference between curved filaments and mature fibrils is due only to the extent of intermolecular β-sheet formation. Because the structure of the rigid, straight, mature fibrils is not compatible with that of the curved, immature fibrils, they cannot be assembled using immature fibrils as precursors. A reasonable interpretation of this structural difference is the parallel organization of the β-strands in the intermolecular β-sheets of the mature fibrils vs. the antiparallel β-sheets in the curved filaments and amorphous aggregates. Gosal et al. [63] in their comprehensive study on the effect of the solution conditions on the fibril formation kinetics and aggregate morphology came to the same conclusion that "worm-like" and "rod-like" short fibrils, which may correspond to the curved immature fibrils and heat induced filaments of this study, form on an off-pathway, but rapid route, that competes with the formation of long-straight fibrils.

Besides its central role in dialysis-related amyloidosis, β2m is a good model protein to study the complex nature of protein aggregation and amyloid formation. Different species of β2m aggregates can be selectively grown by varying the solution conditions. Although the relevance of these aggregates in the progress of dialysis-related amyloidosis is not well understood, the recently proposed role of aggregates different from mature fibrils, such as oligomers and prefibrillar aggregates, in the

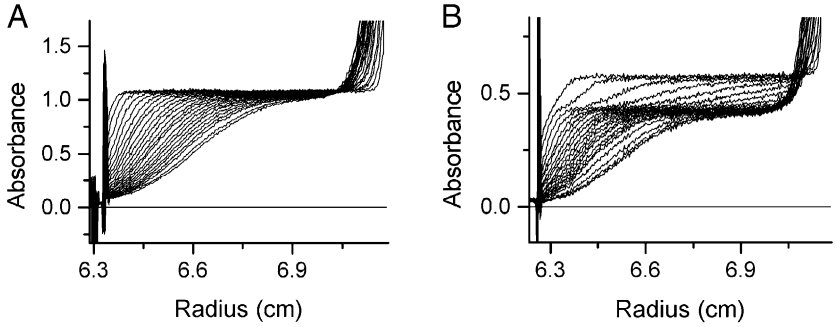

Fig. 7. Ultracentrifuge analysis of native and heat-treated β2m samples at 55,000 rpm. (A) Sedimentation velocity measurement of native β2m at pH 7.5. (B) Sedimentation profile of β2m after 1 h incubation at 75 °C.

process of amyloid diseases [5–9] highlights the importance of such studies.

Acknowledgements

We thank Miyo Sakai (Institute for Protein Research) for the analytical ultracentrifuge experiments and Tomohiko Nakamura (Institute of Scientific and Industrial Research) for the AFM imaging, Prof. Yo Shimizu (Nat. Inst. of Advanced Industrial Science and Technology, Ikeda, Osaka) for his help and Professor Satoshi Takahashi (Institute for Protein Research) for his advices. The work of J. K. was supported by the Japan Society for the Promotion of Science. J. K. is a grantee of the Bolyai János Scholarship of the Hungarian Academy of Sciences.

References

[1] J.C. Rochet, P.T. Lansbury Jr., Amyloid fibrillogenesis: themes and variations, Curr. Opin. Struct. Biol. 10 (2000) 60–68.
[2] J.D. Sipe, Amyloidosis, Annu. Rev. Biochem. 61 (1992) 947–975.
[3] F. Gejyo, T. Yamada, S. Odani, Y. Nakagawa, M. Arakawa, T. Kunitomo, H. Kataoka, M. Suzuki, Y. Hirasawa, T. Shirahama, et al., A new form of amyloid protein associated with chronic hemodialysis was identified as β_2-microglobulin, Biochem. Biophys. Res. Commun. 129 (1985) 701–706.
[4] C.M. Dobson, Protein misfolding, evolution and disease, Trends Biochem. Sci. 24 (1999) 329–332.
[5] M. Stefani, C.M. Dobson, Protein aggregation and aggregate toxicity: new insights into protein folding, misfolding diseases and biological evolution, J. Mol. Med. 81 (2003) 678–699.
[6] K.A. Conway, S.J. Lee, J.C. Rochet, T.T. Ding, R.E. Williamson, P.T. Lansbury Jr., Acceleration of oligomerization, not fibrillization, is a shared property of both α-synuclein mutations linked to early-onset Parkinson's disease: implications for pathogenesis and therapy, Proc. Natl. Acad. Sci. U. S. A. 97 (2000) 571–576.
[7] R. Bhatia, H. Lin, R. Lal, Fresh and nonfibrillar amyloid β protein (1–42) induces rapid cellular degeneration in aged human fibroblasts: evidence for AβP-channel-mediated cellular toxicity, FASEB J. 14 (2000) 1233–1243.
[8] C. Nilsberth, A. Westlind-Danielsson, C.B. Eckman, M.M. Condron, K. Axelman, C. Forsell, C. Stenh, J. Luthman, D.B. Teplow, S.G. Younkin, J. Naslund, L. Lannfelt, The "arctic" APP mutation of (E693G) causes Alzheimer's disease by enhanced Aβ protofibril formation, Nat. Neurosci. 4 (2001) 887–893.
[9] M. Bucciantini, E. Giannoni, F. Chiti, F. Baroni, L. Formigli, J. Zurdo, N. Taddei, G. Ramponi, C.M. Dobson, M. Stefani, Inherent toxicity of aggregates implies a common mechanism for protein misfolding diseases, Nature 416 (2002) 507–511.
[10] J. Floege, M. Ketteler, β_2-Microglobulin-derived amyloidosis: an update, Kidney Int. 59 (2001) S164–S171.
[11] F. Gejyo, M. Arakawa, Dialysis amyloidosis: current disease concepts and new perspectives for its treatment, Contrib. Nephrol. 78 (1990) 47–59.
[12] N. Fujimoto, N. Wada, M. Akiyama, S. Tajima, A. Ishibashi, S. Miyakawa, Coexistence of β_2 microglobulin and λ light chain in amyloid fibrils of dialysis-unrelated plasma cell dyscrasia-associated systemic amyloidosis, Br. J. Dermatol. 147 (2002) 549–553.
[13] N. Fujimoto, M. Yajima, Y. Ohnishi, S. Tajima, A. Ishibashi, Y. Hata, U. Enomoto, I. Konohana, H. Wachi, Y. Seyama, Advanced glycation end product-modified β_2-microglobulin is a component of amyloid fibrils of primary localized cutaneous nodular amyloidosis, J. Invest. Dermatol. 118 (2002) 479–484.
[14] I. Yamaguchi, K. Hasegawa, H. Naiki, T. Mitsu, Y. Matuo, F. Gejyo, Extension of A β2M amyloid fibrils with recombinant human β2-microglobulin, Amyloid 8 (2001) 30–40.
[15] I. Yamaguchi, K. Hasegawa, N. Takahashi, H. Naiki, Apolipoprotein E inhibits the depolymerization of β_2-microglobulin-related amyloid fibrils at a neutral pH, Biochemistry 40 (2001) 8499–8507.
[16] Y. Ohhashi, Y. Hagihara, G. Kozhukh, M. Hoshino, K. Hasegawa, I. Yamaguchi, H. Naiki, Y. Goto, The intrachain disulfide bond of β_2-microglobulin is not essential for the immunoglobulin fold at neutral pH, but is essential for amyloid fibril formation at acidic pH, J. Biochem. 131 (2002) 45–52.
[17] N.M. Kad, S.L. Myers, D.P. Smith, D.A. Smith, S.E. Radford, N.H. Thomson, Hierarchical assembly of β_2-microglobulin amyloid in vitro revealed by atomic force microscopy, J. Mol. Biol. 330 (2003) 785–797.
[18] D. Hong, M. Gozu, K. Hasegawa, H. Naiki, Y. Goto, Conformation of β_2-microglobulin amyloid fibrils analyzed by reduction of the disulfide bond, J. Biol. Chem. 24 (2002) 21554–21560.
[19] D.P. Smith, S. Jones, L.C. Serpell, M. Sunde, S.E. Radford, A systematic investigation into the effect of protein destabilisation on beta 2-microglobulin amyloid formation, J. Mol. Biol. 330 (2003) 943–954.
[20] M. Hoshino, H. Katou, Y. Hagihara, K. Hasegawa, H. Naiki, Y. Goto, Mapping the core of the β_2-microglobulin amyloid fibril by H/D exchange, Nat. Struct. Biol. 9 (2002) 332–336.
[21] T. Chiba, Y. Hagihara, T. Higurashi, K. Hasegawa, H. Naiki, Y. Goto, Amyloid fibril formation in the context of full-length protein: effects of proline mutations on the amyloid fibril formation of β_2-microglobulin, J. Biol. Chem. 278 (2003) 47016–47024.
[22] J. Villanueva, M. Hoshino, H. Katou, J. Kardos, K. Hasegawa, H. Naiki, Y. Goto, Increase in the conformational flexibility of β_2-microglobulin upon copper binding: a possible role for copper in dialysis-related amyloidosis, Protein Sci. 13 (2004) 797–809.
[23] H. Naiki, K. Higuchi, M. Hosokawa, T. Takeda, Fluorometric determination of amyloid fibrils in vitro using the fluorescent dye, thioflavin T1, Anal. Biochem. 177 (1989) 244–249.
[24] H. Naiki, K. Hasegawa, I. Yamaguchi, H. Nakamura, F. Gejyo, K. Nakakuki, Apolipoprotein E and antioxidants have different mechanisms of inhibiting Alzheimer's β-amyloid fibril formation in vitro, Biochemistry 37 (1998) 17882–17889.
[25] H. Naiki, F. Gejyo, Kinetic analysis of amyloid fibril formation, Methods Enzymol. 309 (1999) 305–318.
[26] P. Zavodszky, J.T. Johansen, A. Hvidt, Hydrogen-exchange study of the conformational stability of human carbonic-anhydrase B and its metallo-complexes, Eur. J. Biochem. 56 (1975) 67–72.
[27] P. Zavodszky, J. Kardos, A. Svingor, G.A. Petsko, Adjustment of conformational flexibility is a key event in the thermal adaptation of proteins, Prot. Natl. Acad. Sci. U. S. A. 95 (1998) 7406–7411.
[28] A. Svingor, J. Kardos, I. Hajdu, A. Nemeth, P. Zavodszky, A better enzyme to cope with cold. Comparative flexibility studies on psychotrophic, mesophilic, and thermophilic IPMDHs, J. Biol. Chem. 276 (2001) 28121–28125.
[29] A. Hvidt, S.O. Nielsen, Hydrogen exchange in proteins, Adv. Prot. Chem. 21 (1966) 287–386.
[30] B. Demeler, H. Sabber, J.C. Hansen, Identification and interpretation of complexity in sedimentation velocity boundaries, Biophys. J. 72 (1997) 397–407.
[31] V.J. McParland, N.M. Kad, A.P. Kalverda, A. Brown, P. Kirwin-Jones, M.G. Hunter, et al., Partially unfolded states of β_2-microglobulin and amyloid formation in vitro, Biochemistry 39 (2000) 8735–8746.
[32] N.M. Kad, N.H. Thomson, D.P. Smith, D.A. Smith, S.E. Radford, β_2-microglobulin and its deamidated variant, N17D form amyloid fibrils with a range of morphologies in vitro, J. Mol. Biol. 313 (2001) 559–571.
[33] H. Katou, T. Kanno, M. Hoshino, Y. Hagihara, H. Tanaka, T. Kawai, K. Hasegawa, H. Naiki, Y. Goto, The role of disulfide bond in the amyloidogenic state of β_2-microglobulin studied by heteronuclear NMR, Protein Sci. 11 (2002) 2218–2229.
[34] M. Jackson, H.H. Mantsch, The use and misuse of FTIR spectroscopy in the determination of protein structure, Crit. Rev. Biochem. Mol. Biol. 30 (1995) 95–120.
[35] D.M. Byler, H. Susi, Examination of the secondary structure of proteins by deconvolved FTIR spectra, Biopolymers 25 (1986) 469–487.
[36] L. Narhi, S.J. Wood, S. Steavenson, Y. Jiang, G.M. Wu, D. Anafi, S.A. Kaufman, F. Martin, K. Sitney, P. Denis, J.C. Louis, J. Wypych, A.L.

Biere, M. Citron, Both familial Parkinson's disease mutations accelerate α-synuclein aggregation, J. Biol. Chem. 274 (1999) 9843–9846.
[37] S. Krimm, J. Bandekar, Vibrational spectroscopy and conformation of peptides, polypeptides, and proteins, Adv. Protein Chem. 38 (1986) 181–364.
[38] K.A. Conway, J.D. Harper, P.T. Lansbury Jr., Fibrils formed in vitro from α-synuclein and two mutant forms linked to Parkinson's disease are typical amyloid, Biochemistry 39 (2000) 2552–2563.
[39] A. Dong, W.S. Caughey, Infrared methods for study of hemoglobin reactions and structures, Methods Enzymol. 232 (1994) 139–175.
[40] A. Dong, J. Matsuura, S.D. Allison, E. Chrisman, M.C. Manning, J.F. Carpenter, Infrared and circular dichroism spectroscopic characterization of structural differences between β-lactoglobulin A and B, Biochemistry 35 (1996) 1450–1457.
[41] A.A. Ismail, H.H. Mantsch, P.T.T. Wong, Aggregation of chymotrypsinogen: portrait by infrared spectroscopy, Biochim. Biophys. Acta 1121 (1992) 183–188.
[42] A. Dong, S.J. Prestrelski, S.D. Allison, J.F. Carpenter, Infrared spectroscopic studies of lyophilization- and temperature-induced protein aggregation, J. Pharm. Sci. 84 (1995) 415–424.
[43] F. Gejyo, N. Honma, Y. Suzuki, M. Arakawa, Serum levels of beta 2-microglobulin as a new form of amyloid protein in patients undergoing long-term hemodialysis, N. Engl. J. Med. 314 (1986) 585–586.
[44] K. Yamaguchi, H. Katou, M. Hoshino, K. Hasegawa, H. Naiki, Y. Goto, Core and heterogeneity of β_2-microglobulin amyloid fibrils as revealed by H/D exchange, J. Mol. Biol. 338 (2004) 559–571.
[45] G. Deléage, C. Geourjon, An interactive graphic program for calculating the secondary structures content of proteins from circular dichroism spectrum, Comput. Appl. Biosci. 9 (1993) 197–199.
[46] N. Sreerama, R.W. Woody, Protein secondary structure from circular dichroism spectroscopy. Combining variable selection principle and cluster analysis with neural network, ridge regression and self-consistent methods, J. Mol. Biol. 242 (1994) 497–507.
[47] D.C. Ayers, N.A. Athanasou, C.G. Woods, R.B. Duthie, Dialysis arthropathy of the hip, Clin. Orthop. 290 (1993) 216–224.
[48] C. Van Ypersele, T.B. Drucke, Dialysis Amyloid, Oxford Univ. Press, New York, 1996, pp. 34–68.
[49] S.Y. Tan, M.B. Pepys, Amyloidosis, Histopathology 25 (1994) 403–414.
[50] K. Ono, F. Uchino, Formation of amyloid-like substance from beta-2-microglobulin in vitro. Role of serum amyloid P component: a preliminary study, Nephron 66 (1994) 404–407.
[51] T. Yamada, T. Kakihara, F. Gejyo, M. Okada, A monoclonal antibody recognizing apolipoprotein E peptides in systemic amyloid deposits, Ann. Clin. Lab. Sci. 24 (1994) 243–249.
[52] J.M. Campistol, A. Argiles, Dialysis-related amyloidosis: visceral involvement and protein constituents, Nephrol. Dial. Transplant. 11 (1996) S3:142–S3:145.
[53] T. Kanno, K. Yamaguchi, H. Naiki, Y. Goto, T. Kawai, Association of thin filaments into thick filaments revealing the structural hierarchy of amyloid fibrils, J. Struct. Biol. 149 (2005) 213–218.
[54] F. Chiti, E. De Lorenzi, S. Grossi, P. Mangione, S. Giorgetti, G. Caccialanza, C.M. Dobson, G. Merlini, G. Ramponi, V. Bellotti, A partially structured species of β_2-microglobulin is significantly populated under physiological conditions and involved in fibrillogenesis, J. Biol. Chem. 276 (2001) 46714–46721.
[55] E. De Lorenzi, S. Grossi, G. Massolini, S. Giorgetti, P. Mangione, A. Andreola, F. Chiti, V. Bellotti, G. Caccialanza, Capillary electrophoresis investigation of a partially unfolded conformation of β_2-microglobulin, Electrophoresis 23 (2002) 918–925.
[56] O.N. Antzutkin, J.J. Balbach, R.D. Leapman, N.W. Rizzo, J. Reed, R. Tycko, Multiple quantum solid-state NMR indicates a parallel, not antiparallel, organization of beta-sheets in Alzheimer's β-amyloid fibrils, Proc. Natl. Acad. Sci. U. S. A. 97 (2000) 13045–13050.
[57] T.L. Benzinger, D.M. Gregory, T.S. Burkoth, H. Miller-Auer, D.G. Lynn, R.E. Botto, S.C. Meredith, Propagating structure of Alzheimer's β-amyloid(10–35) is parallel β-sheet with residues in exact register, Proc. Natl. Acad. Sci. U. S. A. 95 (1998) 13407–13412.
[58] M. Balbirnie, R. Grothe, D.S. Eisenberg, An amyloid-forming peptide from the yeast prion Sup35 reveals a dehydrated β-sheet structure for amyloid, Proc. Natl. Acad. Sci. U. S. A. 98 (2001) 2375–2380.
[59] J. Zurdo, J.I. Guijarro, J.L. Jimenez, H.R. Saibil, C.M. Dobson, Dependence on solution conditions of aggregation and amyloid formation by an SH3 domain, J. Mol. Biol. 311 (2001) 325–340.
[60] D.J. Gordon, J.J. Balbach, R. Tycko, S.C. Meredith, Increasing the amphiphilicity of an amyloidogenic peptide changes the β-sheet structure in the fibrils from antiparallel to parallel, Biophys. J. 86 (2004) 428–434.
[61] S. Yamamoto, K. Hasegawa, I. Yamaguchi, S. Tsutsumi, J. Kardos, Y. Goto, F. Gejyo, H. Naiki, Low concentrations of sodium dodecyl sulfate induce the extension of β_2-microglobulin-related amyloid fibrils at a neutral pH, Biochemistry 43 (2004) 11075–11082.
[62] M. Kihara, E. Chatani, M. Sakai, K. Hasegawa, H. Naiki, Y. Goto, Seeding-dependent maturation of β_2-microglobulin amyloid fibrils at neutral pH, J. Biol. Chem. 280 (2005) 12012–12018.
[63] W.S. Gosal, I.J. Morten, E.W. Hewitt, D.A. Smith, N.H. Thomson, S.E. Radford, Competing pathways determine fibril morphology in the self-assembly of β_2-microglobulin into amyloid, J. Mol. Biol. 351 (2005) 850–864.